# Max-Planck-Institut für Meteorologie

*Max Planck Institute for Meteorology*

Report No. 339

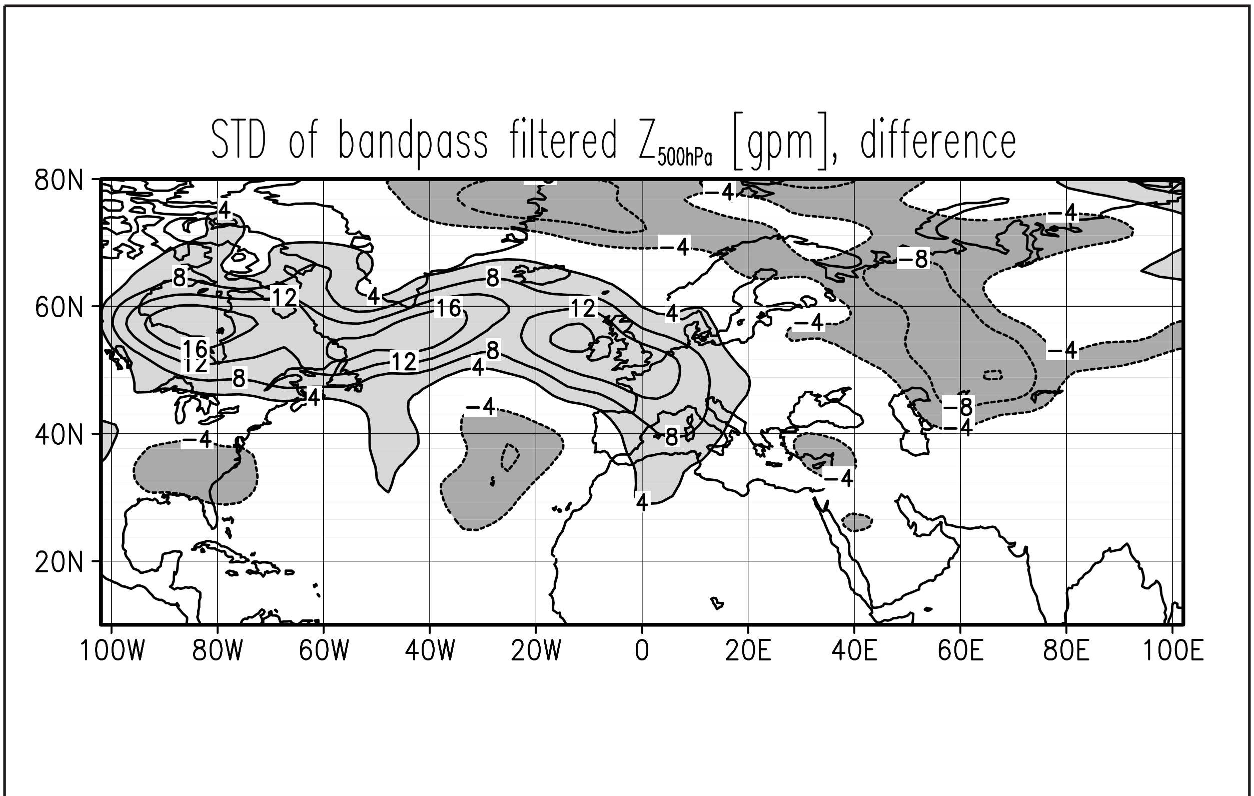


# Modelling the wintertime response to upper tropospheric and lower stratospheric ozone anomalies over the North Atlantic and Europe

by

Ingo Kirchner and Dieter Peters

Hamburg, September 2002

## Authors


Ingo Kirchner — Max-Planck Institut für Meteorologie

Dieter Peters — Leibniz-Institut für Atmosphärenphysik an der Universität Rostock, Kühlungsborn, Germany



Max-Planck-Institut für Meteorologie
Bundesstrasse 55
D - 20146 Hamburg
Germany

Tel.: +49-(0)40-4 11 73-0
Fax: +49-(0)40-4 11 73-298
e-mail: <name>@dkrz.de
Web: www.mpimet.mpg.de



ISSN 0937 - 1060

# Modelling the wintertime response to upper tropospheric and lower stratospheric ozone anomalies over the North Atlantic and Europe

Ingo Kirchner [1] and Dieter Peters [2]

*e-mail: kirchner@dkrz.de, peters@iap-kborn.de*

*submitted to: Annales Geophysicae*

## Contents

**1 Introduction** **3**

**2 Ozone field implementation and the direct radiation effects** **6**

**3 Sensitivity experiments** **9**

**4 Dynamical response** **10**

**5 Summary and discussion** **14**

**A Estimation of 3D ozone fields** **21**

[1]Max-Planck-Institut für Meteorologie, Hamburg, Germany
[2]Leibniz-Institut für Atmosphärenphysik an der Universität Rostock, Kühlungsborn, Germany

**Abstract**

During boreal winter months mean longitude dependent ozone changes in the upper troposphere and lower stratosphere are mainly caused through different ozone transports of planetary waves. The feedback of the changed radiative forcing induced by these ozone changes near the tropopause on the circulation is unclear. This feedback is investigated with the general circulation model ECHAM4 in a sensitivity study.

In the simulation two different mean January realizations of the ozone field are implemented in ECHAM4. Both ozone fields are estimated on the basis of the observed mean January planetary wave structure of the 1980s. The first field represents a 14 year average (reference, 1979-1992) and the second one contains in addition the mean ozone field change (anomaly, 1988-92) in boreal extra-tropics during the end of the 1980s. The model runs were carried out pairwise with identical initial conditions for both ozone fields. Five statistically independent experiments were performed with different sea surface temperatures of the years 1988 to 1992.

The results support the hypothesis, that the zonally asymmetric ozone changes of the 80s triggered a systematic alteration of the circulation over the North Atlantic - European region. It is suggested that this feedback process is important for the understanding of the decadal coupling between troposphere and stratosphere as well as between subtropics and the extra-tropics in winter.

# 1 Introduction

The atmosphere is a complex system with interacting processes of dynamics, radiation and chemistry. For instance the ozone depletion will change the radiative forcing and therefore the whole behaviour of the atmosphere(e.g. Ramaswamy et al., 2001). While the dominant ozone depletion in higher latitudes and higher altitudes seems to be caused by the changed ozone chemistry (WMO, 1999), a large fraction of the decadal changes of zonal mean ozone in the tropopause region of the extra-tropics is dynamically caused.

The longitudinal dependence of the decadal ozone changes is mainly caused by the change of planetary waves as was shown by Hood and Zaff (1995) and Peters et al. (1996) for January of the 1980s. The decadal changes of the zonally asymmetric fields of the atmospheric flow are showing a high anti-correlation between total ozone and tropopause height for mean January (e.g. Schmitz et al., 2000; Steinbrecht et al., 1998). Over Europe a large area of ozone depletion was observed in January of the 1980s, the magnitude was twice as large in its centre as the trend of the zonal mean ozone changes (e.g. McPeters et al., 1996 and Bojkov and Fioletov, 1995). By using a linear transport model, Peters and Entzian (1998) calculated the 3-dimensional decadal ozone changes of the 80s for all winter months, and found they were related to the decadal changes of ultra-long waves. The changes were strongest below the ozone layer maximum (near 70 hPa in mid-latitudes).

Quasi-stationary zonally asymmetric ozone changes may be effected by transport and through photochemical reactions. Both processes operate on different time scales in the tropopause region of the extra-tropics. The transport due to the planetary waves dominates the horizontal ozone distribution in the order of a few days to a month, while the chemical reaction time is much longer. Therefore, changes in the ultra-long waves presumably controlled the large-scale ozone changes (Kurzeja, 1984).

Note, for synoptic waves, Dobson et al. (1929) already knew the connection between anti-cyclonic (cyclonic) flow and low (high) total ozone caused by convergence (divergence) of ozone poor (rich) air in the upper troposphere and lower stratosphere.

Near the tropopause region even small radiative heating (cooling) rates are able to change the radiation balance very efficiently as shown by many model studies using radiative-convective models (e.g. Ramanathan and Dickinson, 1979; Forster and Shine, 1997). For instance Forster and Shine (1997) showed, using the fixed dynamical heating approximation to adjust the stratospheric temperatures, that the temperature change depends significantly on the vertical distribution of the ozone change. Further the authors concluded that the ozone near the tropopause has the greatest influence on the surface temperature. So longitude dependent ozone changes near the tropopause have the potential of coupling the tropospheric and the stratospheric circulation and the subtropics and extra-tropics during winter, because they are in the same order as the zonal mean ozone change. The influence of this radiative forcing over many days or some weeks on the large-scale circulation is not known. Therefore we examine the influence of longitude dependent ozone changes on the large-scale dynamics especially over the North Atlantic - European region during January where these decadal ozone changes were extreme in the 1980s.

A state-of-the-art general circulation model (GCM) like ECHAM4-CHEM as used for time-slice experiments (e.g. Steil et al., 1997) with the full coupling of dynamics, radiation and chemistry involves a high order of complexity. The appearance of many interacting processes makes it hard to verify feedback processes in the GCM. Further, the full coupling of photochemistry and dynamics needs much more computer resources. In addition, the models have to be run for a long time (many years) to get a more realistic and stable climate state.

However the reduction of the complexity from fully coupled models to weakly coupled or un-coupled models (e.g., Austin and Butchard, 1992; Rasch et al., 1995; Stevenson et al., 2000) or the use of models with parameterised chemistry (e.g., Cariolle and Déqué, 1986; Roelofs et al., 1999) are efficient ways to study the link between ozone and circulation. In sensitivity experiments with ozone photochemistry Austin and Butchard (1992) found that the planetary wave activity in mid-latitudes at about 300 hPa strongly modulates the ozone hole variability. Nevertheless, to examine the feedback mechanisms of longitude dependent ozone changes on the circulation, carefully designed sensitivity experiments with a GCM seems to be appropriate.

Note many authors (e.g. Ramaswamy et al., 1996; Hansen et al., 1997; Graf et al., 1998; Langematz, 2000) focused mainly on the climate response of zonally averaged ozone changes which will be explicitly excluded in this study.

As a first step, we used the GCM ECHAM4 including a modified ozone distribution with radiative forcing but without chemistry. The decadal changes of zonally asymmetric ozone in January of the 80s were implemented directly into the radiation code resulting in a model consistent change of radiative forcing. With the known and fixed change of longitude dependent ozone profiles, following the calculations of Peters et al. (1996) (see Appendix) we performed a series of sensitivity experiments. The ozone field implementation and the radiation effects are described in section 2. The experiment design is given in section 3. The results presented in section 4 are focused on the circulation response over the North Atlantic - European region. The results support the hypothesis that the longitudinal asymmetry of ozone changes induces a systematic modification of the circulation over the North Atlantic - European region.

## 2 Ozone field implementation and the direct radiation effects

The 3-dimensional dependence of the January "*reference*" ozone distribution we used in the sensitivity experiments was calculated on the basis of a simplified continuity equation as described in detail in the Appendix. From known mean January fields of geopotential (temperature) and zonal means of zonal velocity (ozone) the longitude dependent ozone field was constructed. The ozone distribution of January 1979 based on satellite measurements (McPeters et al., 1984) was used as a zonal mean ozone distribution of the period 1979-1992. This field includes to some extent the ozone decrease of the years before the 1980s as known from ground based and satellite measurements (e.g. WMO, 1999). But no decadal changes of the zonal mean ozone field of the 80s were included as mentioned in the introduction. Furthermore no longitudinal variability was introduced below 500 hPa and above 70 hPa, and also not in the tropics. The ozone content in those regions is considered adding 45 DU (Dobson Unit), 15 DU for the lower troposphere and 30 DU for the upper stratosphere as known from the estimation of mean ozone profiles. This addition is based on the mean vertical ozone distribution at the station Lindenberg (Feister et al., 1987). The "*reference*" January ozone field has a more realistic geographical distribution in the extra-tropics between 500 and 70 hPa in comparison to the standard ECHAM4 ozone field. The "*anomaly*" ozone field is the superposition of the "*reference*" ozone field and the extra-tropical longitude dependent ozone change only in latitudes north of $30^o N$ to the end of the 1980s. For the uppermost three layers and for some of the lowest layers no change was done explicitly, so that the anomaly was concentrated between the ozone layer maximum and the 500 hPa layer.

The total ozone anomaly as used in the sensitivity experiments is shown in Figure 1a. Fig 1

This anomaly is representing the difference between the ozone field at the end of the 1980s and the "*reference*" field. The total ozone anomaly shows a wave like pattern. The highest positive anomaly was found over the North Atlantic with values up to 10 DU and over Central Europe the value goes down to -10 DU. Secondary ozone maxima exist over North America and around the Kaspian Sea and secondary minima are placed over East Siberia, the Pacific and the western North Atlantic. The height-longitude cross section (not shown) at $50^o\ N$ indicates that the ozone change in the 1980s is concentrated between the tropopause and the ozone layer maximum at about 70 hPa in mid-latitudes.

Note, that the amount of the anomaly is nearly half as large as the observed zonally asymmetric ozone change during the whole decade, especially over Europe (Peters et al., 1996), with other words the introduced total ozone anomaly covers about 50% of the zonally asymmetric observed trend in the 80s.

In order to study the direct net effect of ozone forcing, the solar and thermal heating rates have been estimated simultaneously. This was done by running the radiation code twice, first, with the "*reference*" ozone field for January, and then including the ozone anomaly. The difference of the heating rates measures the instantaneous (direct) radiative forcing of the ozone anomaly without any feedback. In Figure 1b(c) the solar (thermal) radiation forcing in the layer of it's maximum is shown based on a ten day average. The solar forcing shows a weak cooling over Europe and a heating over the North Atlantic ocean at 150 hPa. The thermal forcing shows a weak heating over Europe and a cooling over the North Atlantic at 70 hPa. For both a large-scale structure with zonal wave-numbers 3 to 4 dominates, consistent with the ozone difference (anomaly) field shown in Figure 1a. Fig 2

Furthermore, to examine the vertical structure of the forcing, the height-latitude cross Fig 3 section of positive (negative) ozone anomaly over the North Atlantic (European) sector is shown representing a zonal average between $40^o\ W$ and $10^o\ W$ (Fig 2) ($0^o$ and $30^o\ E$ (Fig 3). In part (a) of Figures 2 and 3 the ozone anomaly and in part (b) of Figures 2 and 3 the net heating rate change are plotted from level 13 near 700 hPa to the model top. The solar heating change is given in part (c) of Figures 2 and 3 and the thermal heating rate change in part (d) of Figures 2 and 3, respectively.

Over the eastern North Atlantic (Fig 2), the positive ozone anomaly centered at about 150 hPa in mid-latitudes causes a narrow net heating slightly shifted to the equator. It is reduced poleward due to the missing solar radiation over the winter pole. The solar radiation and the thermal radiation rate contribute both to the net forcing below the 100 hPa layer. But the cooling due to the thermal radiation dominates in mid-latitudes above the 100 hPa layer. Both effects together tend to decrease the lapse rate near the tropopause region.

In the European sector (Fig 3) the negative ozone anomaly is shifted northward in comparison to the location of the positive ozone anomaly over the North Atlantic (see Fig 2). A narrow net cooling follows in mid-latitudes below the 100 hPa layer (dominated by the solar radiation) and heating above (thermal radiation dominates). Therefore, over Europe, the vertical structure of the forcing tends to increase the lapse rate in the tropopause region.

Both examples demonstrate the regional and altitude dependent change of sign of the ozone anomaly forcing: Heating (cooling) in the upper troposphere corresponds to cooling (heating) in the lower stratosphere over the North Atlantic (Europe). Such weak forcing of locally only up to 0.01 K/day can have a strong effect on the stability near the tropopause (e.g. Forster and Shine, 1997). This forcing systematically reduces the thermal stability in the upper troposphere near the tropopause over the North

Atlantic and increases the stability over Europe. The magnitude of the heating/cooling is weak, but the induced three dimensional stability changes could amplify the net heating/cooling of the atmosphere due to feedback processes. These feedbacks can only be investigated by model simulations as discussed in the following. Note the meridional gradient between subtropical and middle latitudes near the tropopause (below 100 hPa) is weakened over the North Atlantic and enhanced over Europe (not shown). Also the heating (cooling) causes upper level divergence (convergence), leading a tendency of the surface pressure to decrease (increase).

# 3 Sensitivity experiments

The sensitivity experiments were performed with the GCM ECHAM4 using T42 horizontal resolution and 19 vertical levels up to 10 hPa. A detailed description of the model physics was given by Roeckner et al. (1996). The starting conditions of the GCM experiments are taken from the standard ECHAM4 AMIP run (see Stendel and Bengtsson, 1997) for five different years (1988, 1989, 1990, 1991, 1992) at the first of October. For each pair the sea surface temperature field was also taken from the AMIP2 data set of the corresponding winter.

In the experiments the ozone field implementation was changed in comparison to the standard ECHAM4 version (see section 2). With the two reconstructed ozone distributions pairwise wintertime experiments were performed. Both ozone fields were initially preprocessed on pressure levels and on a $5 \times 5^o$ grid followed by an interpolation onto the horizontal grid of ECHAM during the initialisation. At every time step the vertical interpolation to the hybrid levels of the model was performed. During this vertical transformation the ozone column integral was conserved. First of all we adjusted the model dynamics to the "*reference*" ozone field and ran the model from the beginning of October until the end of November for each of the five statistically independent time slices. After the first of December we ran the model twice. In the so called "reference" experiment we continued the free ECHAM4 run over two months until the end of January without any further alterations of the ozone. In the so called "anomaly" experiment we are using the "*anomaly*" ozone field without any further changes. The difference between the "*reference*" and the "*anomaly*" ozone field is relatively small and exists per definition only in middle and high northern latitudes. Hence a 30 day adjustment of the dynamics is sufficient. Both data pools ("reference" and "anomaly" experiment) with 5 independent Januaries were analysed and the results are presented in the next section. The observed longitude dependent decadal ozone changes in December and January are quite similar (Peters and Entzian, 1998). Therefore the composed January ozone fields can be used also for the full experiment period.

# 4 Dynamical response

First of all we are interested in a possible global response, visible in the fields of hydrodynamics and thermodynamics which are caused by the large-scale ozone anomaly in extra-tropics of the Northern Hemisphere in January. For our diagnostics the meridional velocity as an indicator of the planetary wave structure in combination with temperature were chosen. The difference between the ensemble means ("anomaly" minus "reference" experiment) of the meridional velocity and the temperature at the 200 hPa layer are shown in Figure 4. The amplitudes are in the order of $\pm\, 5\ m/s$ and $\pm\, 1.5\ K$ respectively. The difference pattern shows a large-scale wave like structure (with wave number 1-6) on both hemispheres organised as wave tracks. Fig 4

One track appears in northern mid-latitudes, beginning over the western North Atlantic, passing Europe and ending over Asia. An other track is starting at the same region but is moving southwards to Africa. A third wave track occurs in the Southern Hemisphere. It starts over the subtropical eastern South Pacific ocean, passing South America, the South Atlantic and Africa, and ending over the Indic. A comparison of significant changes of meridional velocity with temperature changes shows that significance in both fields only appears in the extra-tropics.

By including also the 100 hPa layer results and the vorticity and divergence of 500 hPa, 200 hPa, 100 hPa, 70 hPa (not shown) we find three regions of significant (local T-test) changes. The first one is the North Atlantic-European region, the second area the North Polar region and the third one a is band from South America to South Africa (SA2 region for short). The larger areas of significance over the SA2 region are connected to a weaker large-scale wave variability during the austral summer as known from global analysis (e.g. Randel, 1992).

We focus on the North Atlantic-European region where the ozone anomaly dominates (Fig 1) and examine the dynamics in more detail. There exists a strong Rossby wave track also in the difference field of geopotential height, relative vorticity and zonal wind at 200 hPa (Fig 5). The track starts over the subtropical middle North Atlantic indicated by a trough and follows a curvature in an anti-cyclonic sense. That means a course given further by an high pressure system northwards of the Azores and a Black Sea low. Consistent with that, the changes of vorticity (Fig 5b) and zonal wind (Fig 5c), showing positive (negative) values on the northward (southward) side of the anti-cyclone, are also statistically significant (95%). Fig 5

The temperature difference field in 200 hPa (see Fig 5c) shows a strong cooling of about $-1.5\ K$ in connection with the high northwards of the Azores and an increase of about $1.5\ K$ northwards of the Faroyer Islands, as well as over the Black Sea region in connection with low pressure systems. The significant temperature change is mainly linked to adiabatic cooling in the upper troposphere (heating in the lower stratosphere) of ascent (descent) air.

We continue the large-scale diagnostics by a calculation of the longitude extended Eliassen-Palm flux vector changes as suggested by Plumb (1985) (for short called Plumb flux). The stationary wave difference of the sample averages ("anomaly" minus "reference") was calculated and then the corresponding Plumb flux was estimated. In 250 hPa (Fig 6a) for the extra-tropics of the North Atlantic, an upward flux mainly directed eastward is found, and over Europe a stronger southeastward component occurs. The strong flux changes over the subtropical North Atlantic are not considered because the used geostrophic approximation for flux calculation is only valid in extra-tropics. Fig 6

To study the height-longitude behaviour, an average over the latitude band $40^o\ N - 60^o\ N$ was calculated. It shows (Fig 6b) a feature which is concentrated over the North Atlantic-European region with a strong upward-eastward component over the eastern North Atlantic and a strong downward-eastward component over Europe. The convergence near the surface between $40^oW$ and $20^oW$ is dominated by a strong differential vertical heat flux. In the tropopause region (near 300 hPa), also in the same longitude band, a convergence is found as a result of strong differential vertical heat flux and meridionally momentum flux. A large divergent area occurs over Europe at about 300 hPa with higher wave activity which could decelerate the zonal mean wind (Plumb, 1985). The projection of 3-dimensional Plumb flux structure onto the 200 hPa layer is in good agreement with the planetary wave track described above.

For the propagation as well as for the reflection of ultra-long waves in a basic stream the wave-wave interaction between quasi-stationary waves plays an important role. But transient eddies are also known to have an important effect on the longitude dependent circulation (e.g. Trenberth, 1986; Hoskins et al., 1983; Fraedrich et al., 1993).

A 2-6 days filter of daily values (deviation from the monthly mean) is used for the analyses of transient eddies. The high-pass structure change of these eddies is studied by estimating the extended Eliassen Palm flux after Trenberth (1986) as a difference of the ensemble means of both experiment pools.

In 250 hPa (Fig 7a) a strong upward-eastward flux contribution is found over East Canada and western North Atlantic. The lower track orbits to the south and is oriented downwards over the middle subtropical North Atlantic. The upper track is more zonally and passes Europe. A latitude band average ($40^o\ N - 60^o\ N$) shows clearly an height-longitude structure concentrated over the North Atlantic- European region. Strong upward-eastward eddy heat flux occurs westwards of $40^o\ W$ with a strong momentum flux in the tropopause region which extends eastwards over Europe. The horizontal divergence of the eddy flux vector shows three centres of possible longitude dependent basic stream deceleration $90^o\ W - 50^o\ W$, $30^o\ W - 15^o\ W$, $3^o\ E - 13^oE$ and two larger regions of acceleration $50^o\ W - 30^o\ W$ and $15^o\ W - 3^o\ E$. Fig 7

The storm-track activity (2-6 days bandpass filtered 500 hPa geopotential height field) defined as the standard deviation of the bandpass filtered field is correlated to the mean cyclone tracks (e.g. Trenberth, 1991). In Figure 8 the January average of the storm-track variability for the “reference” and the “anomaly” experiment are shown and agrees well with eddy flux estimations of Figure 7. The difference (Fig 8c) shows a clear signal which is linked to the northward shift of the jet stream over the Atlantic (see Fig 5c). Fig 8

In the ozone “anomaly” runs the cyclonic activity is enhanced on the north-western and northern flank of its centre and over the south-eastern area of the North Atlantic storm-track. In addition on the eastern side (over East Europe) the cyclone activity will be less spread and reduced. This stronger barrier effect is expected from 200 hPa geopotential height field change over the North Atlantic (centred at eastern side) and over northern Russia where anti-cyclonic disturbances occur (Fig 5a). Fig 9

The enhanced geopotential height variance in 500 hPa occurs in a band over the North Atlantic, over a line between negative and positive geopotential height (1000 hPa) changes (Fig 9a). This fact is known from observations of North Atlantic variability like the North Atlantic oscillation (NAO) (e.g. Hurrel, 1995; Hastenrath and Greischar, 2001). The positive mean geopotential height anomaly (at 1000 hPa) whose centre is placed over a region northwards of the Azores Islands (about 40 gpm) correlates on its northern flank with more cloud cover percentage and more liquid water content (Fig 9b and c), but on its southern flank with less in both quantities. The precipitation (Fig 9d) decreases over the region of the anti-cyclonic disturbances. All these patterns agree quite well with observations of positive NAO phase realisations (Thompson and Wallace, 2001).

# 5 Summary and discussion

In this sensitivity study a simple estimation of the large-scale three dimensional ozone change of the 1980s during January was introduced. The ozone fields describe the right phase locations and vertical ozone profiles in the extra-tropics of the Northern Hemisphere as observed. The sensitivity experiments show that the zonally asymmetric ozone changes in the upper troposphere and lower stratosphere (north of $30^o\ N$) induced a systematic modification of the circulation.

Three significant wave tracks were found, two occur over the North Atlantic and one over the South Atlantic. Further the results show a statistically significant response over three large regions, namely over the North Atlantic-European, Arctic and SA2 region.

It can be concluded that the ozone changes with related relative weak radiative forcing near the tropopause are important for the coupling between troposphere and stratosphere and also between the subtropics and the extra-tropics during boreal winter decades.

We looked for a very efficient feedback mechanism including planetary waves, storm tracks, convective activity and water vapour. The instantaneous radiative forcing due to the ozone anomaly (see Figures 1, 2 and 3) alone can not explain the strong response over the North Atlantic. Therefore we analysed the difference of the radiative forcing terms of the temperature tendency equation for mean January conditions. In the heating rate difference of the dynamically balanced state the signature of the ozone anomaly was found in the solar part near 150 hPa (Fig 10a) and upward (c). The heating area agrees well with more ozone in this height region over the North Atlantic. This additional ozone causes a primary decreasing of the lapse rate near the tropopause (Fig 2), the convection will reach higher levels, and more water vapour will cause additional solar heating. Note without dynamics this heating would be balanced due to the counteracting emission of long wave radiation and the thermal heating increases too. Fig 10

The model results at 150 and 100 hPa show a different large-scale distribution of mean January difference in thermal forcing (Fig 10b and d) dependent on the action of dynamics, but also a factor of 10 larger than the direct thermal forcing induced by the ozone change. Both forcings together described the total radiative forcing for mean January conditions and this is one order larger than the total instantaneous radiative forcing through the ozone change.

In summary the sensitivity study confirms that small ozone anomalies near the tropopause result in a stronger effect on the stability as expected from instantan forcing due to positive feedbacks. This steered the cyclonic activity over the North Atlantic as shown in our results and induced the reported planetary wave structure changes.

To focus on the North Atlantic-European region where the ozone changes are largest the model results show a realistic physical picture of atmospheric circulation changes as known from many observational studies of decadal circulation changes especially in the 1980s (e.g. Hurrel, 1995).

The mean ozone anomaly structure, typical for the end of the 1980s, is correlated with an enhanced NAO positive phase with a stronger Azores high and weaker Icelandic low at the surface. The mean ozone anomaly induced in the model a similar pattern near the surface (Fig 9a) and that could enhance the dynamical variability in the North Atlantic-European region especially. The location of the storm tracks is shifted to the north and they intensify. Therefore the divergence of the induced transient eddies will force the jet stream shift and produce quasi-stationary waves changes too.

Over the Arctic region also a statistical significant dynamical response is found. This can be explained by an intensification of transient wave activity in mid-latitudes which forces quasi-stationary waves propagating upward and northward into the polar stratosphere. The waves are filtered and reflected by the polar jet so that a large-scale wave with wavenumber one is dominant.

There are open questions which should be studied in the future. So the robustness of this result should be checked in other model configurations. Further, the locally significant area over SA2 region could be forced directly over the Atlantic by Rossby wave propagation through a westerly wind guide (“westerly ducts”) over the tropical West Atlantic (not shown). The frequency of such Rossby wave breaking events is highest during the northern winter (Waugh and Polvani, 2000). On the other hand, in the southern summer, the large scale variability over the Southern Hemisphere mid-latitudes is relatively weak so that a significant response would be easier to detect. Some similar experiments with linear enhanced ozone anomaly show an amplified response but a different structure with high variability in the North Atlantic-European region. That means carefully designed experiments are necessary to detect some threshold values. Further studies should also include the effect of the zonal mean ozone trend and the middle atmosphere.

## Acknowledgements.

The authors would like to thank H. Voß for estimating the Plumb and Trenberth flux vectors. Also the support from W. Randel for providing the update of the NCAR dataset and by NSSDC for making available TOMS-data is gratefully acknowledged. The software package GrADS made by B. Doty are used for all figures. For the improvement of the manuscript we thank A. Gabriel, H.-F. Graf, E. Roeckner and G. Schmitz.

# References

Austin, J. and Butchart, N.: 1992, A three–dimensional modeling study of the influence of planetary wave dynamics on polar ozone photochemistry, *Journal of Geophysical Research* **97**(D9), 10,165–10,186.

Bojkov, R. and Fioletov, V.: 1995, Estimating the global ozone characteristics during the last 30 years, *Journal of Geophysical Research* **100**(D8), 16,537–16,551.

Cariolle, D. and Déqué, M.: 1986, Southern hemisphere medium-scale waves and total ozone disturbances in a spectral general circulation model, *Journal of Geophysical Research* **91**(D10), 10,825–10,846.

Dobson, G., Harrison, D. and Lawrence, J.: 1929, Measurements of the amount of ozone in the earth's atmosphere and its relation to other geophysical conditions, *Proc. R. Soc. Lodon* **A.122**, 456–486.

Feister, U., Plessing, P. and Grasnick, K.: 1987, Vertical ozone distribution over lindenberg (52.22 n, 14.12 e), 1975-82, *Geodaet. Geophys. Veröff. II* **28**, 49–95.

Forster, P. M. de F. and Shine, K. S.: 1997, Radiative forcing and temperature trends from stratospheric ozone changes, *Journal of Geophysical Research* **102**(D9), 10841–10855.

Fraedrich, K., Bantzer, C. and Burkhardt, U.: 1993, Winter climate anomalies in Europe and their associated circulation at 500 hpa, *Climate Dynamics* **8**(4), 161pp.

Graf, H.-F., Kirchner, I. and Perlwitz, J.: 1998, Changing lower stratospheric circulation: The role of ozone and greenhouse gases, *Journal of Geophysical Research* **103**, 11,251–11,261.

Hansen, J., Sato, M. and Ruedy, R.: 1997, Radiative forcing and climate response, *Journal of Geophysical Research* **102**(D6), 6831–6864.

Hastenrath, S. and Greischar, L.: 2001, The north atlantic oscillation in the NCEP-NCAR Reanalysis, *Journal Climate* **14**, 2402–2413.

Hood, L. and Zaff, D.: 1995, Lower stratospheric stationary waves and the longitude dependence of ozone trends in winter, *Journal of Geophysical Research* **100**(D12), 25,791–25,800.

Hoskins, B. J., James, I. N. and White, G. H.: 1983, The shape, propagation and mean-flow interaction of large-scale weather systems, *Journal of Atmospheric Sciences* **40**, 1595–1612.

Hurrel, J. W.: 1995, Decadal trends in the North Atlantic oscillation: regional temperatures and precipitation, *Science* **269**, 676–679.

Kurzeja, R. J.: 1984, Spatial variability of total ozone at high latitudes in winter, *Journal of Atmospheric Sciences* **41**, 695–697.

Langematz, U.: 2000, An estimate of the impact of observed ozone losses on stratospheric temperatures, *Geophysical Research Letters* **27**(14), 2077–2080.

McPeters, R. D., Keath, D. F. and Bhortia, P. K.: 1984, Average ozone profiles for 1979 from NIMBUS 7 SBUV instrument, *Journal of Geophysical Research* **89**, 5199–5214.

McPeters, R., Hollandsworth, S., Flynn, L., Herman, J. and Seftor, C.: 1996, Long-term ozone trends derived from the 16-year combined Nimbus 7/Meteor 3 TOMS Version 7 record, *Journal of Geophysical Research* **23**(25), 3699–3702.

Peters, D. and Entzian, G.: 1998, Longitude-dependent decadal changes of total ozone in boreal winter months during 1979-92, *Journal Climate* **12**, 1038–1048.

Peters, D., Entzian, G. and Schmitz, G.: 1996, Ozone anomalies over the North Atlantic-European region during January 1979-1992 - Linear modelling of horizontal and vertical ozone transport by ultra-long waves, *Contributions to Atmospheric Physics* **69**(4), 477–489.

Plumb, R. A.: 1985, On the three-dimensional propagation of stationary waves, *Journal of Atmospheric Sciences* **42**, 217–229.

Ramanathan, V. and Dickinson, R. E.: 1979, The role of stratospheric ozone in the zonal and seasonal radiative energy balance of the Earth troposphere system, *Journal of Atmospheric Sciences* **36**, 1084–1104.

Ramaswamy, V., Schwarzkopf, M. and Randel, W.: 1996, Fingerprint of ozone depletion in the spatial and temporal pattern of recent lower-stratospheric cooling, *Nature* **382**(6592), 616–618.

Ramaswamy, V. and et al.: 2001, Stratospheric temperature trends: Observations and model simulations, *Reviews of Geophysics* **39**, 71–122.

Randel, W.: 1992, Global atmospheric circulation statistics 1000-1 mb, NCAR technical note NCAR/TN-366+STR.

Rasch, P., B.A.Boville and G.Brasseur: 1995, A three-dimensional general circulation model with coupled chemistry for the middle atmosphere, *Journal of Geophysical Research* **100**, 9041–9071.

Roeckner, E., Arpe, K., Bengtsson, L., Christoph, M., M. Claussen and, L. D., Esch, M., Giorgetta, M., Schlese, U. and Schulzweida, U.: 1996, The atmospheric general circulation model ECHAM-4: Model description and simulation, of the present-day climate, *Report 218*, Max–Planck–Institut für Meteorologie, Hamburg.

Roelofs, G., Lelieveld, J. and Feichter, J.: 1999, Model simulations of the changing distribution of ozone and its radiative forcing of climate: past, present and future, *Report 283*, Max–Planck–Institut für Meteorologie, Hamburg.

Schmitz, G., Peters, D. and Entzian, G.: 2000, Tropopause pressure change in January during 1979-1992, *Meteorologische Zeitschrift Neue Folge* **9**(5), 255–261.

Steil, B., Dameris, M., Brühl, C., Crutzen, P., Grewe, V., Ponater, M. and Sausen, R.: 1997, Development of a chemistry module for GCMs: First results of a multi-annual integration, *Annales Geophysicae*. Report 74 DLR Publication.

Steinbrecht, W., Claude, H. and Köhler, U.: 1998, Correlation between tropopause height and total ozone: implication for long-term changes, *Journal of Geophysical Research* **103**, 19183–19192.

Stendel, M. and Bengtsson, L.: 1997, Toward monitoring the tropospheric temperature by means of a general circulation model, *Journal of Geophysical Research* **102**(D25), 29779–29788.

Stevenson, D. S., Johnson, C. E., Collins, W. J., Derment, R. G. and Edwards, J. M.: 2000, Future estimates of tropospheric ozone radiative forcing and methane turnover - the impact of climate change, *Geophysical Research Letters* **27**(14), 2073–2076.

Thompson, D. and Wallace, J.: 2001, Regional climate impacts of the northern hemisphere annular mode, *Science* **293**, 85–88.

Trenberth, K. E.: 1986, An assessment of impact of transient eddies on the zonal flow during a blocking episode using focalized Eliassen-Palm diagnostics, *Journal of Atmospheric Sciences* **43**, 2070–2087.

Trenberth, K. E.: 1991, Storm tracks in the southern hemisphere, *Journal of Atmospheric Sciences* **48**, 2159–2178.

Waugh, D. W. and Polvani, L. M.: 2000, Climatology of intrusion into the tropical upper troposphere, *Geophysical Research Letters* **27**, 3857–3860.

WMO: 1999, Global ozone research and monitoring project - scientific assessment of ozone depletion: Geneva 1998, Report No. 44.

# A Estimation of 3D ozone fields

The linearised stationary equation for the mass mixing ratio of a zonally asymmetric tracer $\eta^*$ neglecting source terms reads (following Peters et al., 1996)

$$\frac{[U]}{a\cos\varphi}\frac{\partial\eta^*}{\partial\lambda} = -\frac{v^*}{a}\frac{\partial[\eta]}{\partial\varphi} - w^*\frac{\partial[\eta]}{\partial Z} \tag{1}$$

$$Z = -H\ln(\frac{p}{p_s}) \tag{2}$$

where Z is the vertical coordinate, $\lambda$ the longitude and $\varphi$ the latitude. p is the pressure and $p_s$ = 1000 hPa. (U,v,w) represents the velocity components. [...] means zonally averaged values and a star deviations from them.

In the extra-tropics quasi-geostrophic relations holds:

$$v^* = \frac{1}{af\cos\varphi}\frac{\partial\phi^*}{\partial\lambda} \tag{3}$$

$$w^* = \dot{Z}^* = -\frac{1}{N^2}\left(\frac{[U]R}{aH\cos\varphi}\frac{\partial T^*}{\partial\lambda} - \frac{[U]_Z}{a\cos\varphi}\frac{\partial\phi^*}{\partial\lambda}\right) \tag{4}$$

$\phi$ is the geopotential, f the Coriolisparameter, a the earth radius and T the temperature. (4) is the linearised version of the stationary energy equation but without a diabatic heat source term. The thermal wind equation, $T_\varphi R$ = -a H $U_Z$ , was introduced; $\varphi$ and Z indices are derivatives. $N^2$ was height and latitude dependent. The used constants are H = 7.321 km, a = 6.37 $\cdot$ $10^3$ km, $\rho = \rho_0 e^{-Z/H}$ with $\rho_0$ = 1.225 kg/m$^3$, R = 287 m$^2$/K/s$^2$. (3) and (4) inserted in (1) gives the continuity equation in a form where the geopotential and temperature appear explicitly. The zonally asymmetric resolution was realised by a Fourier decomposition and calculated numerically as vertical profiles at 14 layers from 500 hPa to 10 hPa.

The observed amplitudes and phases of the geopotential, temperature and zonal mean fields were taken from the mean January values of Randel (1992). The zonal mean ozone distribution of January 1979 is based on data from McPeters et al. (1984) for NIMBUS7 SBUV instrument. A check and discussion of the model results are also given in Peters et al. (1996).

# List of Figures


1 Ozone anomaly and direct radiation forcing at 70 hPa . . . . . . . . . . 23

2 Ozone anomaly and radiation forcing zonally averaged (40$^o$W - 10$^o$W) 24

3 Ozone anomaly and radiation forcing zonally averaged (0 - 30$^o$E) . . 25

4 Meridional wind and temperature response at 200 hPa . . . . . . . . . . 26

5 Geopotential height, vorticity and zonal wind response at 200 hPa . . 27

6 Stationary flux changes over the North Atlantic . . . . . . . . . . . . 28

7 Transient flux changes over the North Atlantic . . . . . . . . . . . . . . 29

8 Storm track variability at the 500 hPa layer . . . . . . . . . . . . . . . 30

9 Ozone anomaly response . . . . . . . . . . . . . . . . . . . . . . . . . . 31

10 Ozone anomaly forcing with feedbacks . . . . . . . . . . . . . . . . . 32

**a)**

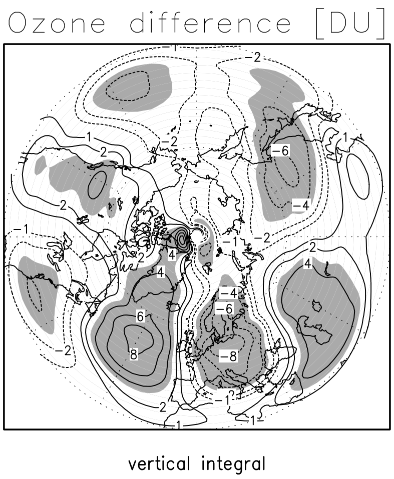


**b)**

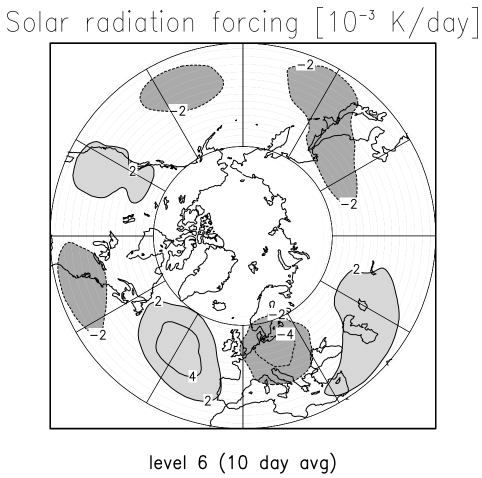


**c)**

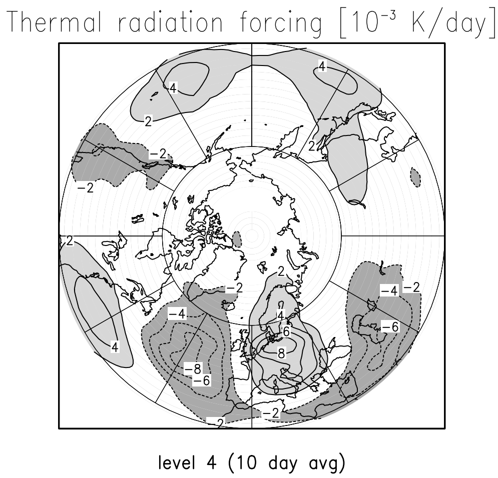


Figure 1:

Ozone anomaly and direct radiation forcing estimated under January conditions averaged over 10 days:

**a)** Vertically integrated ozone difference

**b)** Solar radiation forcing due to the ozone difference at 150 hPa (model level 6)

**c)** Same as b) but for the thermal radiation at 70 hPa (model level 4)

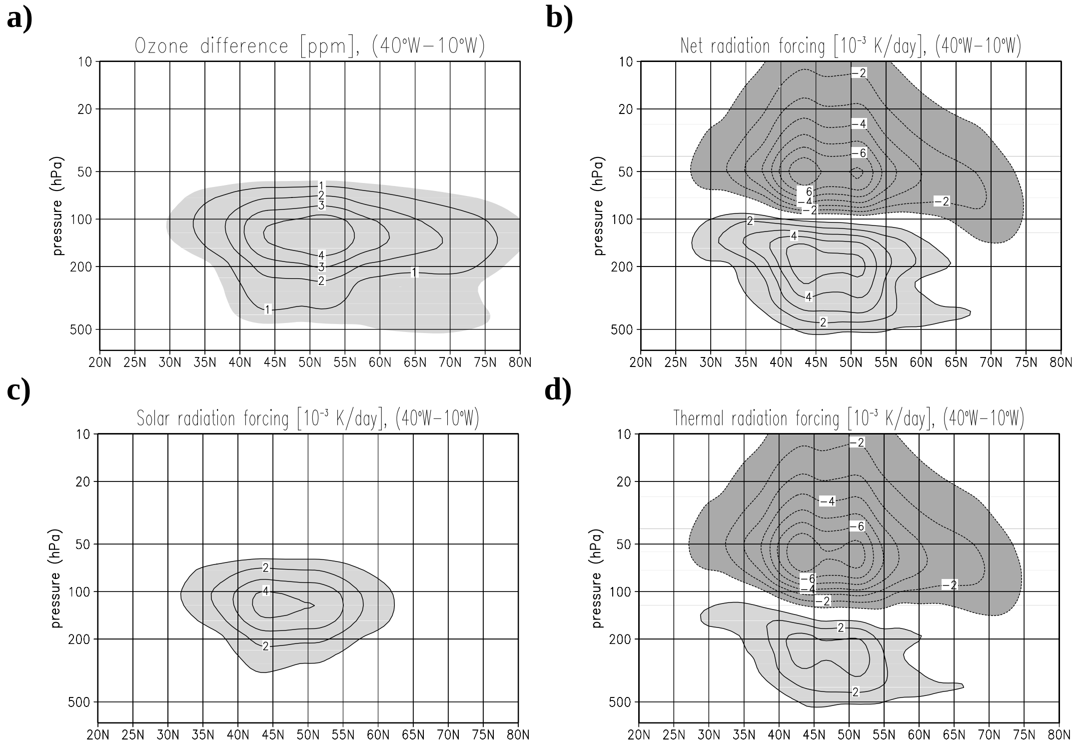


Figure 2:
Zonally averaged (40$^o$W - 10$^o$W) vertical distribution of the ozone anomaly and radiation forcing of January averaged over 10 days

**a)** Ozone difference

**b)** Net radiation heating due to the ozone difference

**c)** Same as b) but only solar radiation heating

**d)** Same as b) but only thermal radiation heating

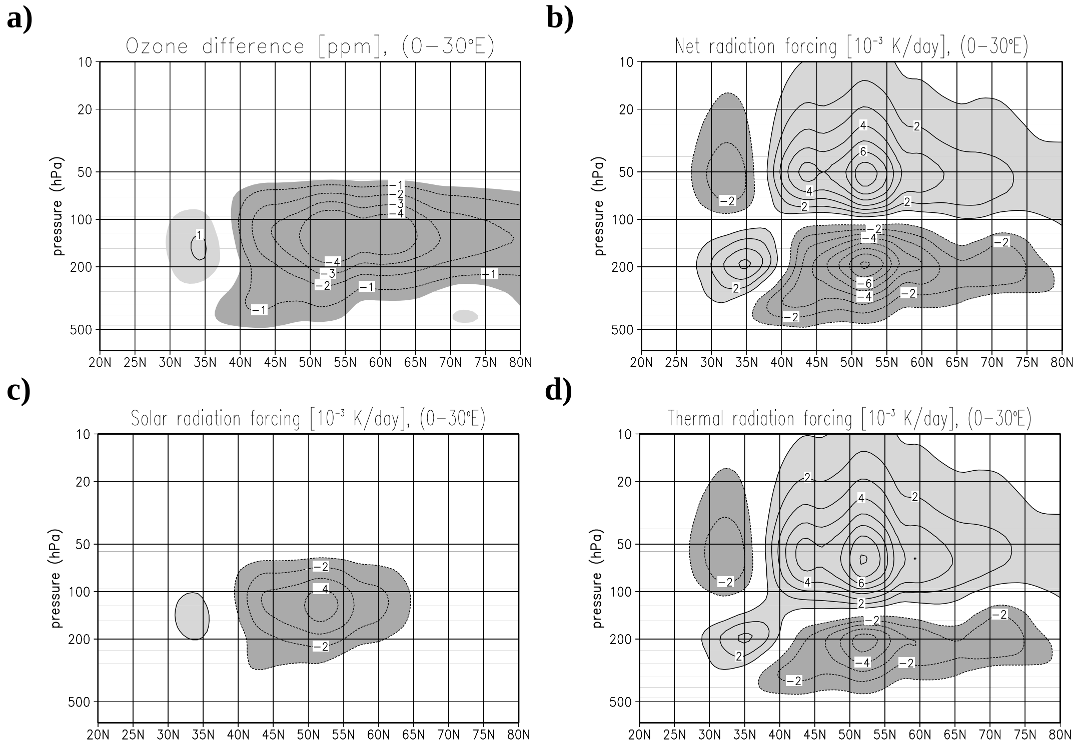


Figure 3:
Same as in Figure 2, but zonally averaged (0 - 30$^o$E)

**a)**

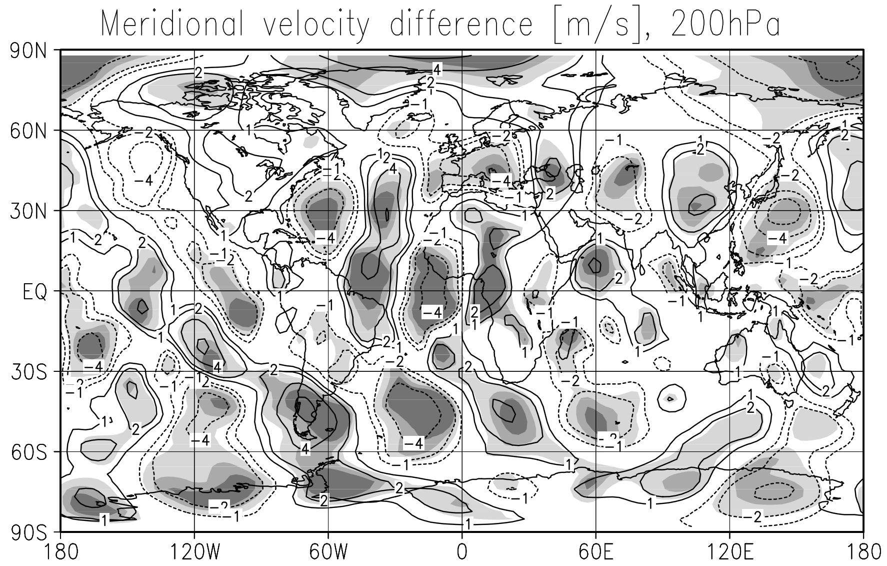


**b)**

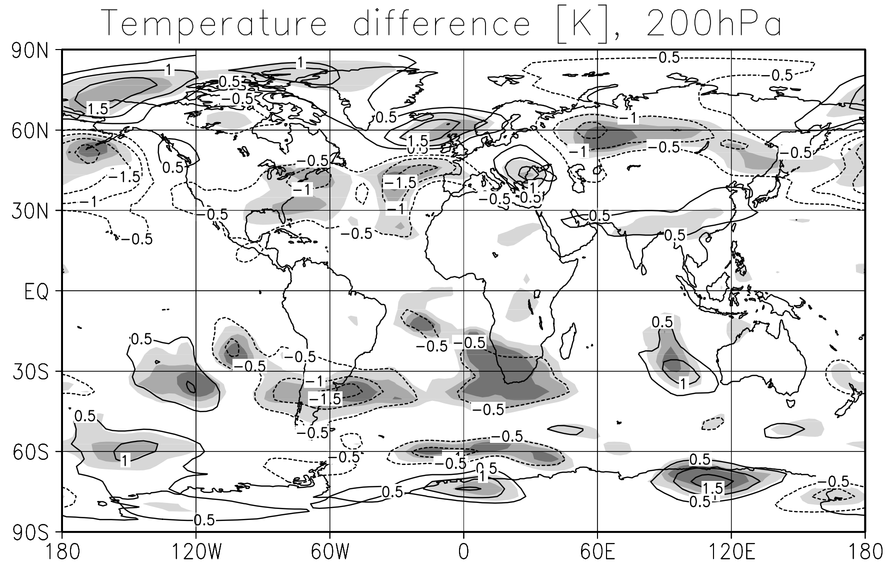


Figure 4:
Mean meridional wind (a) and temperature (b) response at 200 hPa, regions inside a significance level of 80% (light), 90% (middle) and 95% (dark) are shaded

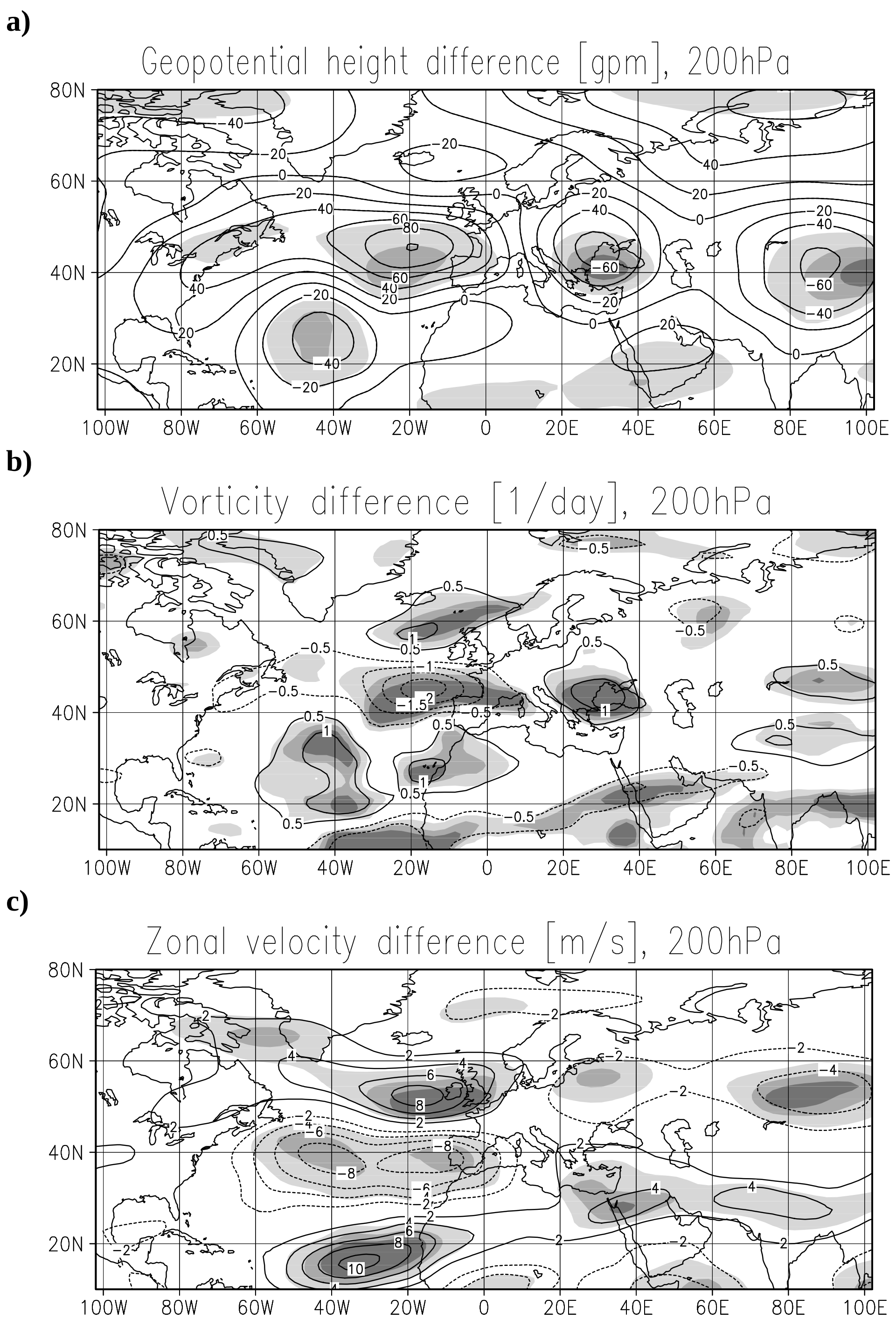


Figure 5:
Mean geopotential height (a), vorticity (b) and zonal wind (c) response at 200 hPa for the North Atlantic-European region, shading as in Figure 4

**a)**

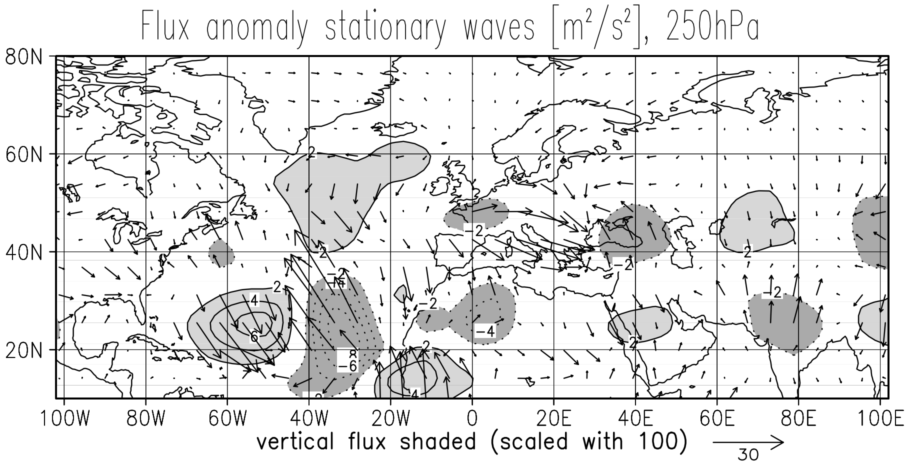


**b)**

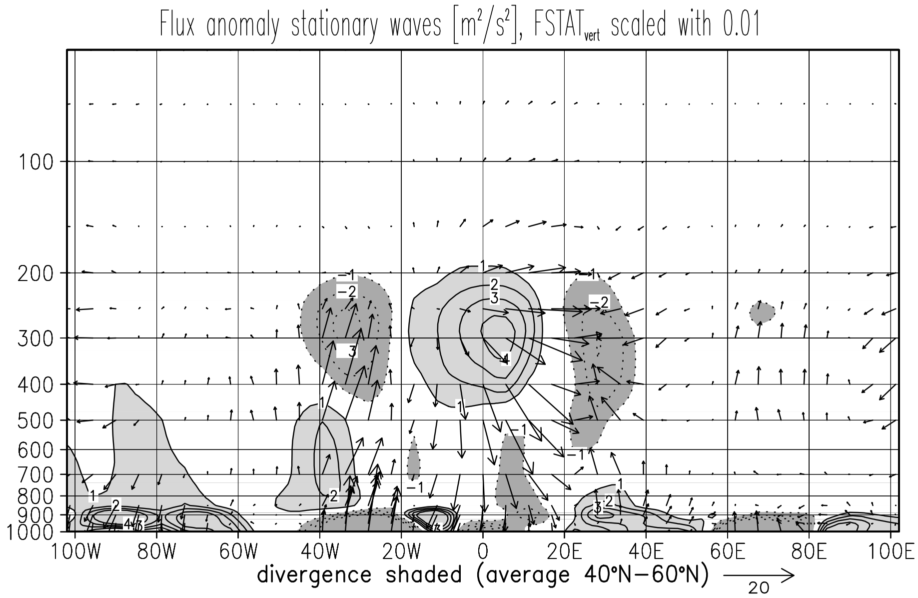


Figure 6:
Stationary flux changes (Plumb, 1985) over the North Atlantic due to the ozone anomaly

**a)**

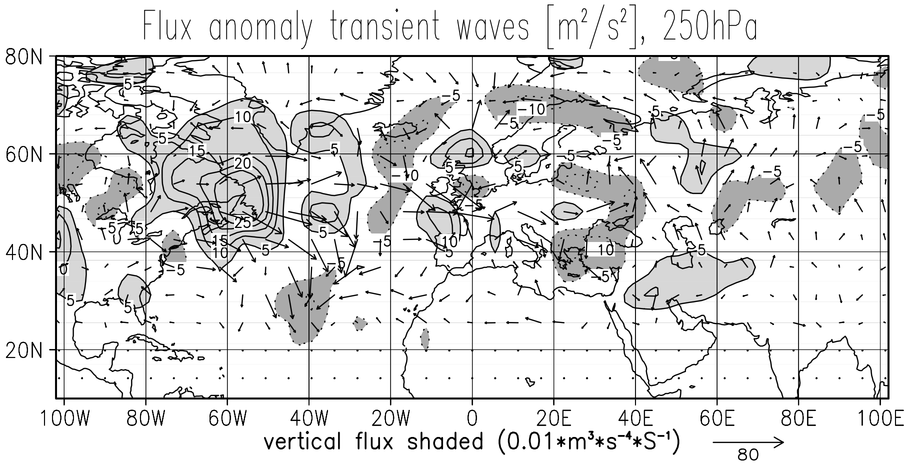


**b)**

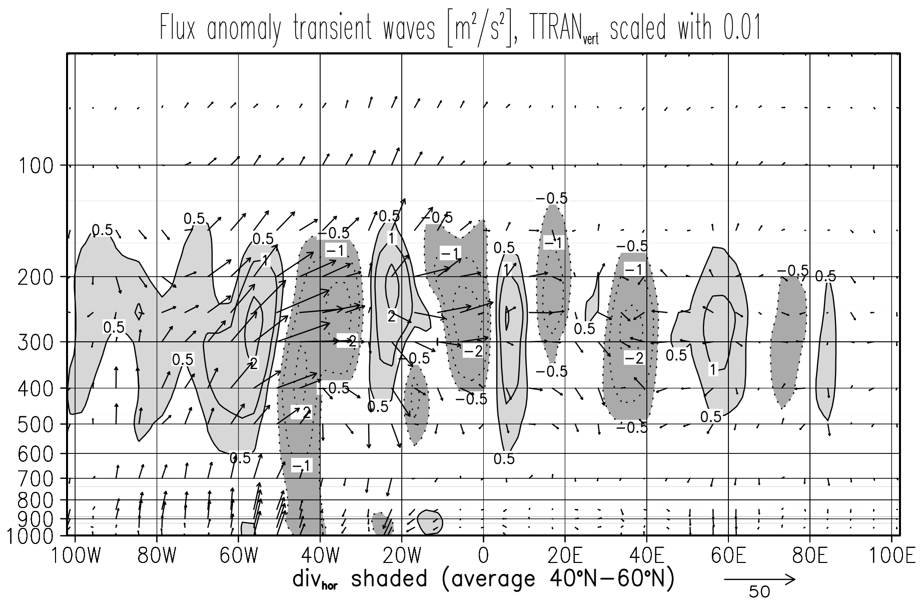


Figure 7:
Transient flux changes (Trenberth, 1986) over the North Atlantic due to the ozone anomaly for a high pass filtered flow (2-6 days)

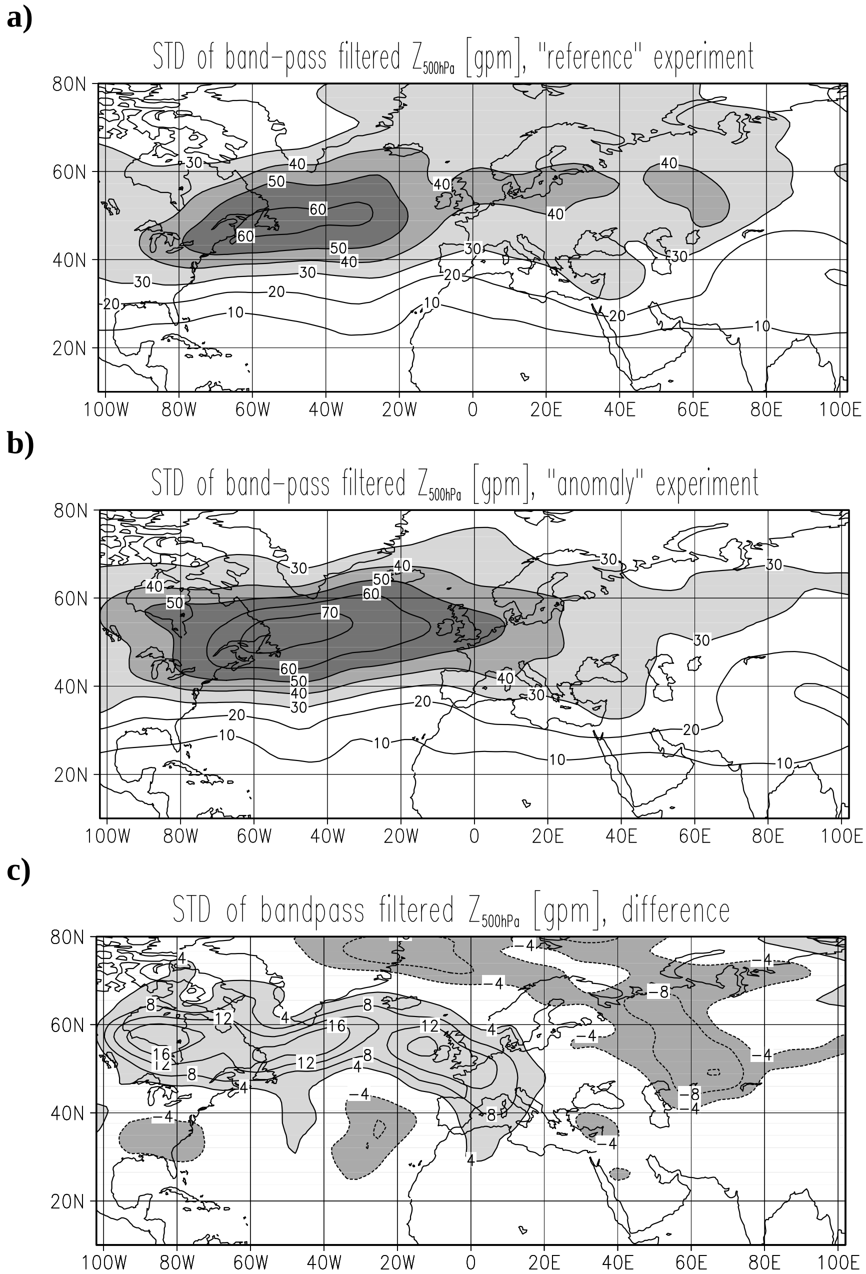


Figure 8:
Storm track variability at the 500 hPa layer for mean January

**a)** Variance of the band pass filtered (2-6 days) geopotential height at the 500 hPa for the “reference” experiment

**b)** Same as a) but for the “anomaly” experiment

**c)** Difference between “anomaly” and “reference” experiment

**a)**

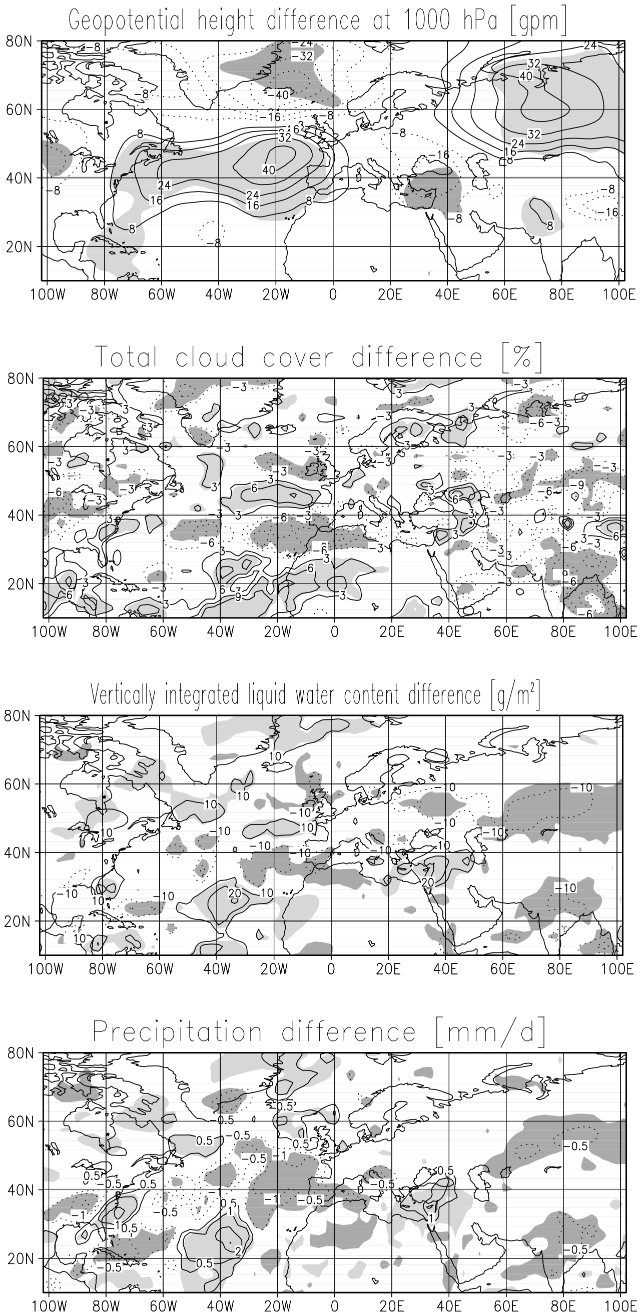


Figure 9:
The ozone anomaly response for mean January as difference field (regions inside a significance level of 80% are shaded)

**a)** For geopotential height at 1000 hPa

**b)** For total cloud cover

**c)** For vertical integrated liquid water

**d)** For precipitation

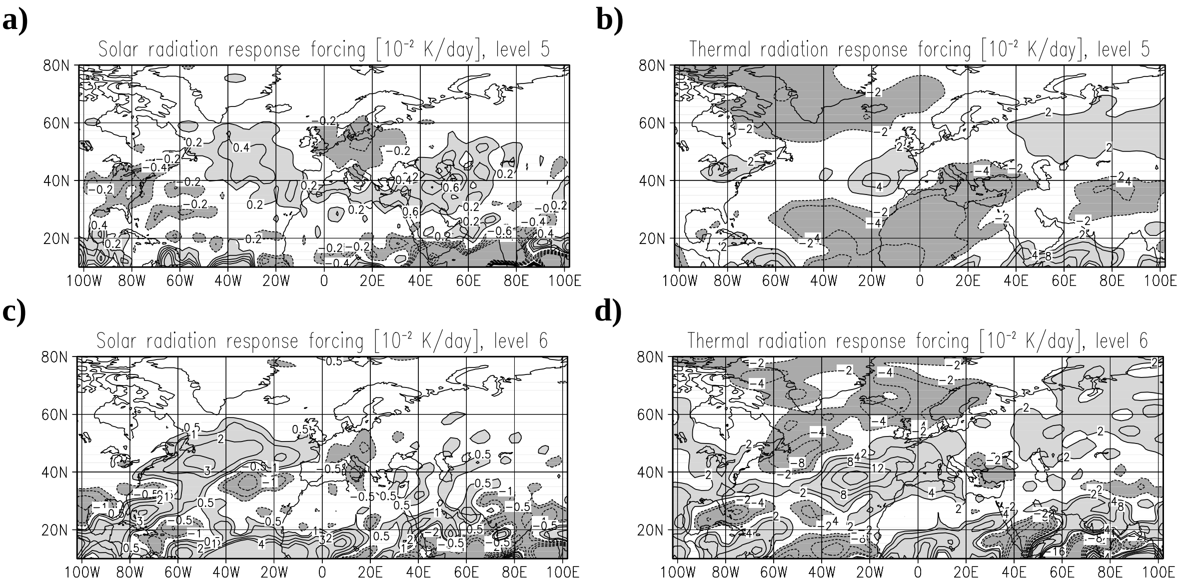


Figure 10:
Mean January forcing difference due to ozone anomaly including dynamical feedbacks (positive values light shaded, negative values dark shaded)

**a)** For solar radiation at level 5 (near 100 hPa)

**b)** For thermal radiation same level as a)

**c)** For solar radiation at level 6 (near 150 hPa)

**d)** For thermal radiation same level as c)